ASTRONOMY & ASTROPHYSICS
SUPPLEMENT SERIES

Astron. Astrophys. Suppl. Ser. **71**, 63-67 (1987)

The identification of galactic radio sources based on a comparison of radio-continuum and infrared emission

E. Fürst ([1]), W. Reich ([1]) and Y. Sofue ([2])

([1]) Max-Planck-Institut für Radioastronomie, Auf dem Hügel 69, 5300 Bonn 1, F.R.G.
([2]) Department of Astronomy, University of Tokyo, Bunkyo-ku, Tokyo 113, Japan

Received March 27, accepted April 23, 1987

Summary. — The ratio of the far-infrared to the radio continuum emission is very different for HII regions and supernova remnants. Using the IRAS 60 μm and radio 2.7 GHz emission it is demonstrated that this difference provides an effective tool to distinguish between thermal and non-thermal sources even in highly confused regions in the Galactic plane.

Key words : infrared emission — radio continuum emission — HII regions — supernova remnants.

1. Introduction.

The Galactic radio emission near the Galactic plane shows up as a mixture of mainly thermal HII regions and non-thermal supernova remnants (SNRs) superposed on a smooth ridge of « background » emission. The identification of the physical nature of these sources is often based on studies of spectral indices derived from observations at several radio wavelengths, on radio polarization measurements or on supporting optical observations.

A comparison of radio continuum surveys with the recently published sky flux product of the Infrared Astronomical Satellite (IRAS) mission (Beichmann *et al.*, 1985) provides a new method to separate non-thermal and thermal sources. According to Emerson and Jennings (1978) HII regions radiate most of their energy in the infrared (IR). The ratio (R) of IR to radio continuum flux density is about $R \approx 1000$. Supernova remnants are much weaker IR emitters ($R \lesssim 15$; Braun, 1986). The high contrast in R can be used to identify sources even in highly confused regions.

We have compared the IRAS 60 μm survey with the Effelsberg 2.7 GHz survey (Reich *et al.*, 1984) to investigate the nature of galactic sources. Both surveys seem to be quite suitable for this purpose : they have similar angular resolution (4.'27 at 2.7 GHz and 4'-6' at 60 μm) and a high dynamic range. Compared with radio continuum surveys at higher frequencies the 2.7 GHz data have a higher fraction of non-thermal emission, while 60 μm is close to the peak wavelength of the IR emission of HII regions.

In this paper we present the general procedure to compare both surveys. The detailed investigation of various sources will be reported elsewhere.

2. The method of comparison between the infrared (IR) and the radio data.

The investigation of the IR and radio data is based on the 60 μm data (HCON1, scaled in surface brightness units of Jy/ster) and the 2.7 GHz Galactic plane survey (scaled in mK T_B). As has been pointed out by Reich *et al.* (1984) the radio continuum survey is not corrected for the large-scale Galactic temperature gradient. The diffuse background emission seen in the IRAS maps is still affected by the zodiacal emission. In order to compare the different maps for small-scale sources (HII regions, SNRs, etc.) the diffuse emission of a scale $\gtrsim 1°$ in both maps has been removed by using the « background filtering (BGF) » technique (Sofue and Reich, 1979) in a slightly modified way : we have excluded strong compact sources from the algorithm (see the paper by Sofue and Reich). The removed large-scale emission may consist of several components : diffuse galactic emission, unresolved small scale sources, and in case of the far-infrared emission some contribution of zodiacal emission.

After subtraction of the diffuse background the maps have been convolved to a half power beam width

Send offprint requests to : E. Fürst.

(HPBW) of 6′. The inspection of the responses of the different telescopes to strong compact sources revealed only small differences. Finally, the maps have been scaled to mJy/beam of the 2.7 GHz main beam (HPBW = 4.′27) at 2.7 GHz ($\Sigma_{2.7\,\mathrm{GHz}}$) and at 60 μm ($\Sigma_{60\,\mu\mathrm{m}}$). As an example we show the area $25° \leq \ell \leq 31°$, $|b| \leq 1°5$ (Fig. 1(a) for 2.7 GHz, and Fig. 1(b) for 60 μm).

A first inspection of the two maps shows that all known SNRs in the plotted area (G27.4 + 0.0, G27.8 + 0.6, G29.7 − 0.3, G30.7 + 1.0) are not visible in the 60 μm map, while known HII regions are visible in both maps (note that the radio data are plotted in mJy/beam and the 60 μm data in Jy/beam). For the known SNRs $R < 10$, in case of HII-regions R clusters around $R = 1000$. Both values are in agreement with the results of Emerson and Jennings (1978) for HII regions and of Braun (1985) for SNRs. This large difference in the IR/radio continuum ratio, if it is generally true for all SNRs, can be used for a global search for SNRs even in confused areas.

To present the non-thermal emission more clearly we subtracted the IR map from the 2.7 GHz map to obtain the difference map $\Delta\Sigma(\mathrm{mJy/beam}) = \Sigma_{2.7\,\mathrm{GHz}} - \Sigma_{60\,\mu}/1000$. HII regions should cluster around zero in this difference map. Positive values corresponding to $R < 1000$ are presented in figure 2(a), negative values ($R > 1000$) are shown in figure 2(b). In figure 2(a) we have marked all objects known to have nonthermal radio spectra. In agreement with the detected ratio $R(< 10)$ for the known SNRs they are visible in figure 2(a). The other features may be also non-thermal or thermal sources with $R \lesssim 1000$.

In order to separate the two types of objects we have divided the difference map (Fig. 2(a, b)) by the radio continuum map (Fig. 1(a)) and get a ratio $\eta = \Delta\Sigma/\Sigma_{2.7\,\mathrm{GHz}} \equiv 1 - R/1000$. The ratio η has been estimated only if the 2.7 GHz flux density ≥150 mJy/beam in order to avoid division by values close to zero.

A preliminary analysis of HII regions yields a distribution of η peaked on $\eta = 0$ and a half width of $\Delta\eta \approx 1$ corresponding to a variation of R between $R = 500$ and $R = 1500$. A detailed analysis of η for HII regions is in progress.

The ratio η of the known SNRs is close to $\eta = 1$ as expected from the detected value of $R(\leq 10)$. In figure 3 we plotted all features with $\eta \geq 0.75$. All sources not identified as SNRs have to be considered as candidates for SNRs and will be subject to further investigation.

3. Conclusion.

The comparison of IR and radio continuum data as described above can be used as an effective method to separate thermal and non-thermal objects in radio continuum surveys. The detection limit of non-thermal objects is about 150 mJy/beam in regions with negligible HII emission (after subtraction of the Galactic large-scale emission). This limit corresponds to a surface brightness of $\Sigma_{2.7\,\mathrm{GHz}} \approx 10^{-21}\,\mathrm{W\,m^{-2}\,Hz^{-1}\,ster^{-1}}$. In areas with significant HII emission superposed on SNRs a ratio $\eta < 1.0$ will result. In this case more sophisticated methods (removing of local base levels, differential temperature plots) are required.

Different ratios of IR to radio continuum of HII regions are often interpreted in terms of variations in the amount of dust and as an indication of different H_c^+/H^+ ratios. The IRAS data and the 2.7 GHz survey present the most sensitive measurements to date and allow the examination of the IR/radio continuum variation of HII regions with unprecedented accuracy.

Acknowledgements.

We would like to thank an anonymous referee for several helpful comments.

References

Beichmann, C. A., Neugebauer, G., Habing, H. J., Clegg, P. E. and Chester, T. J. : 1985, IRAS Explanatory Supplement.
Braun, R. : 1985, Doctoral Thesis, Sterrewacht Leiden.
Emerson, J. P., Jennings, R. E. : 1978, *Astron. Astrophys.* **69,** 129.
Reich, W., Fürst, E., Steffen, P., Reif, K., Haslam, C.G.T. : 1984, *Astron. Astrophys. Suppl. Ser.* **58,** 197.
Sofue, Y., Reich, W. : 1979, *Astron. Astrophys. Suppl. Ser.* **38,** 251.

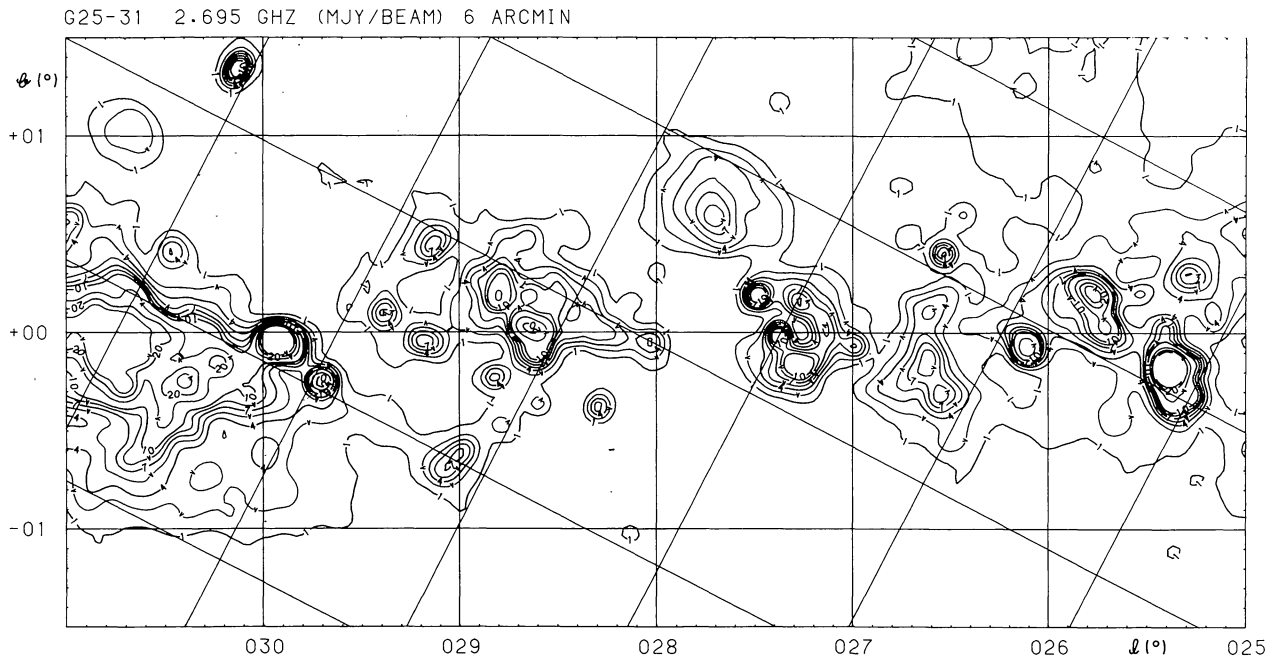

FIGURE 1(a). — Contour plot of the Galactic emission at 2.7 GHz after subtraction of large-scale a emission ($\gtrsim 1°$). Contours are in steps of 150 mJy/beam beginning at 100 mJy/beam (labelled 1) up to 1000 mJy/beam (labelled 10) and further in steps of 500 mJy. The angular resolution is 6′.

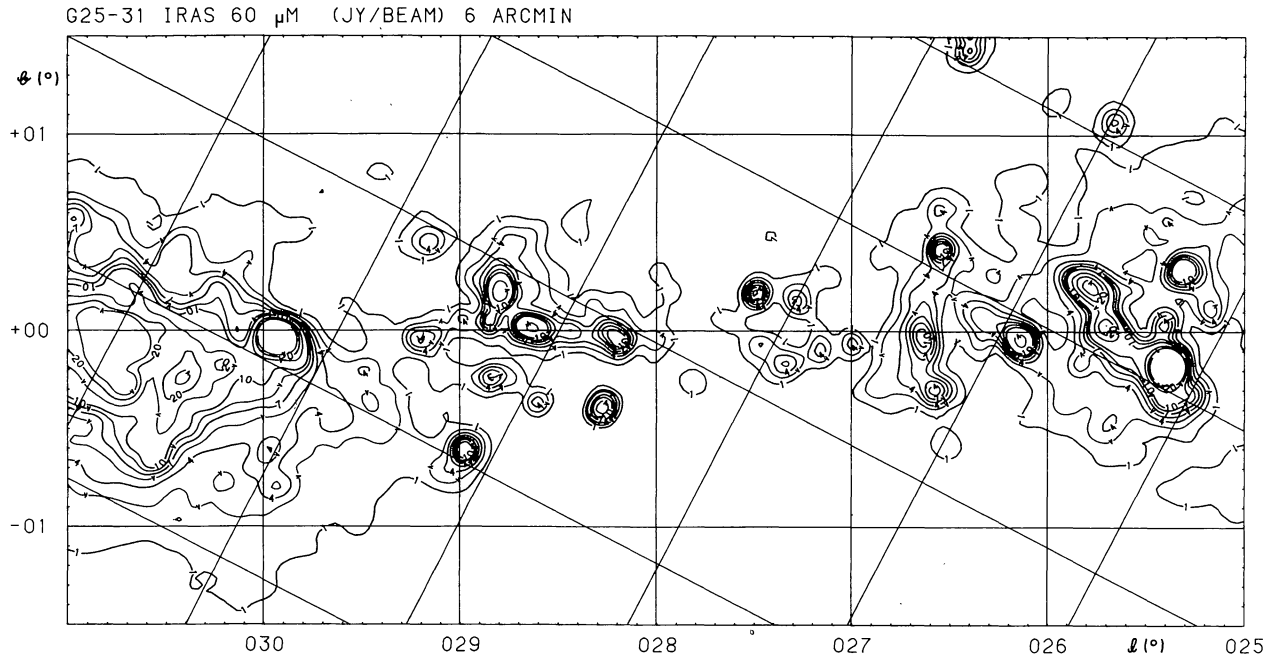

FIGURE 1(b). — Contour plot of the Galactic emission at 60 μm after subtraction of the large-scale emission ($\gtrsim 1°$). Contours are as in figure 1(a) but in Jy/beam instead of mJy/beam. The angular resolution is 6′.

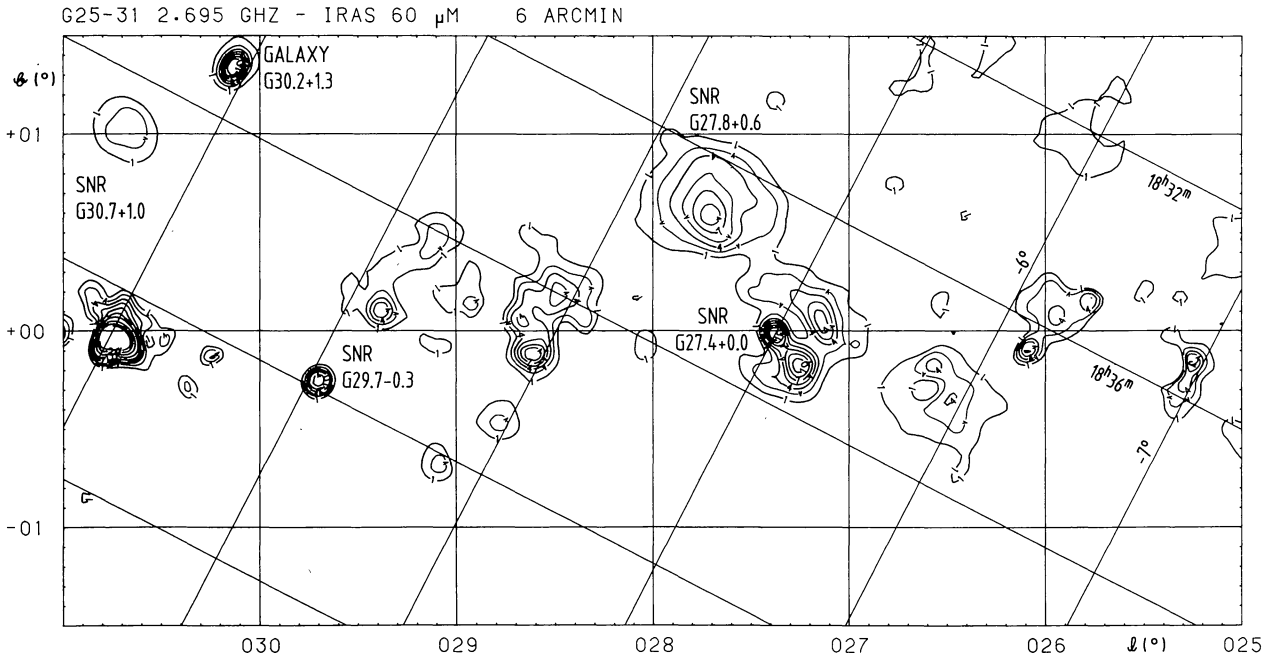

FIGURE 2(a).

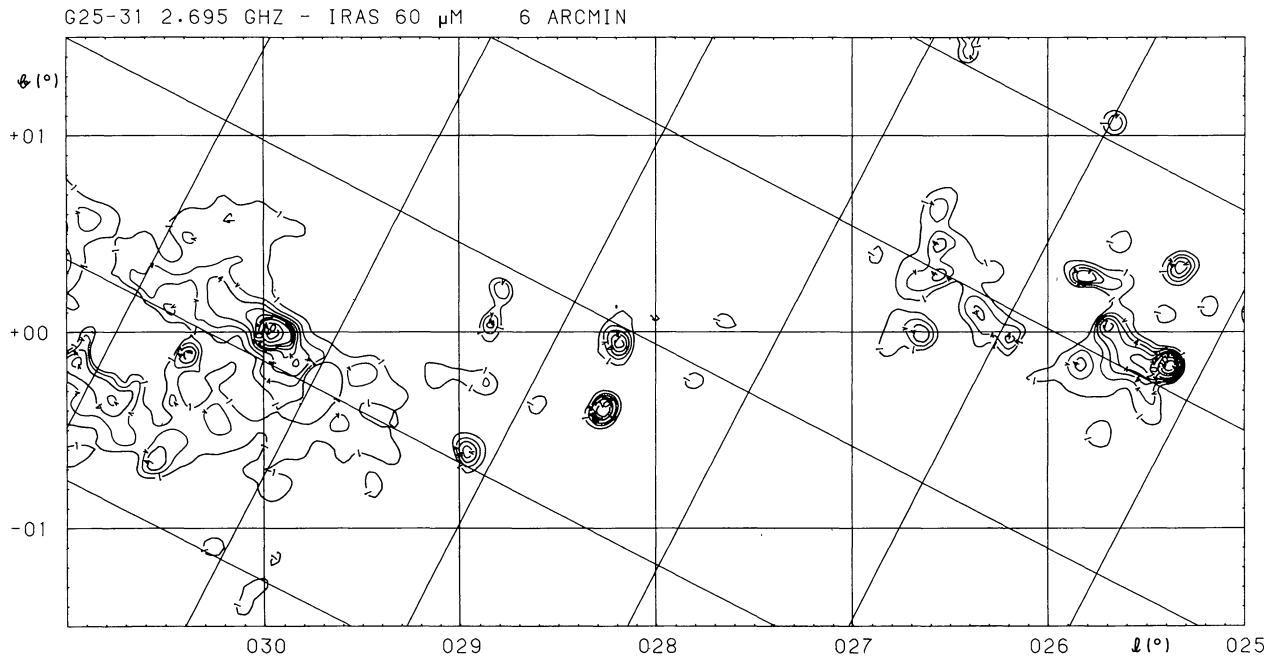

FIGURE 2(b).

FIGURE 2. — The difference map $\Delta\Sigma$ between the 2.7 GHz (Fig. 1(a)) and the 60 μm ($\times$ 0.001) (Fig. 1(b)) emission. (a) We have chosen the same absolute contour values as in figure 1(a). This figure shows the « radio bright » sources. Identified non-thermal objects are marked by their Galactic coordinates. (b) Negative contours in the same intervals as in figure 2(a). This figure shows the « infrared bright » sources.

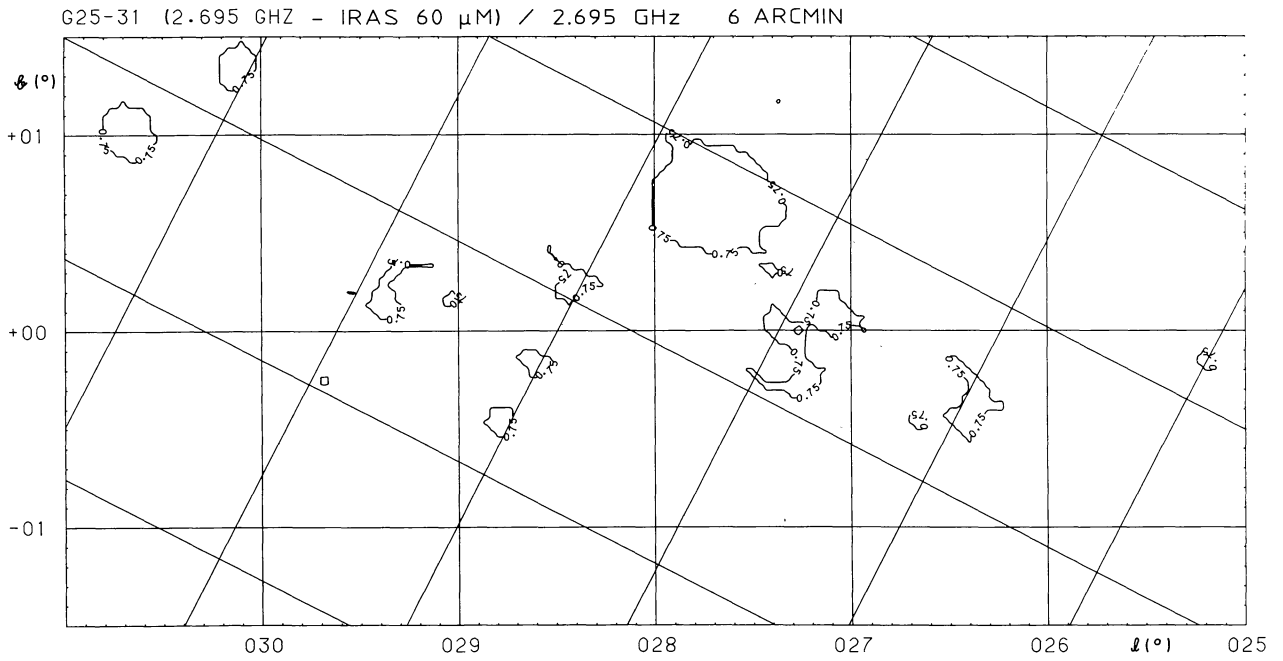

FIGURE 3. — Plot of contour 0.75 of the ratio η of the emission difference (Fig. 2(a)) and the radio continuum map (Fig. 1(a)). This contour encloses areas of emission from likely non-thermal objects.